Contribution of a bioenergetics model to investigate the growth and survival of European seabass in the Bay of Biscay – English Channel area

Chloé Dambrine[a],[*], Martin Huret[a], Mathieu Woillez[a], Laure Pecquerie[b], François Allal[c], Arianna Servili[d], Hélène de Pontual[a]

[a] *Ifremer, Laboratoire de Biologie Halieutique, Unité de Sciences et Techniques Halieutiques, Centre Ifremer Bretagne, ZI de la Pointe du Diable – CS 10070, Plouzané 29280, France*
[b] *Univ Brest, CNRS, IRD, Ifremer, LEMAR, Plouzané F-29280, France*
[c] *MARBEC, Univ Montpellier, CNRS, Ifremer, IRD, Palavas-les-Flots, France*
[d] *Ifremer, Univ Brest, CNRS, IRD, LEMAR, Plouzané F-29280, France*

ABSTRACT

The European seabass (*Dicentrarchus labrax*) is a species of particular ecological and economic importance. Stock assessments have recently revealed the worrying state of the "Northern stock", probably due to overfishing and a series of poor recruitments. The extent to which these poor recruitments are due to environmental variability is difficult to assess, as the processes driving the seabass life cycle are poorly known. Here we investigate how food availability and temperature may affect the growth and survival of wild seabass at the individual scale. To this end, we developed a bioenergetics model based on the Dynamic Energy Budget (DEB) theory. We applied it to seabass population of the Northeast Atlantic region (Bay of Biscay – English Channel area) throughout their entire life cycle. We calibrated the model using a combination of age-related length and weight datasets: two were from aquaculture experiments (larvae and juveniles raised at 15 and 20°C) and one from a wild population (juveniles and adults collected during surveys or fish market sampling). By calibrating the scaled functional response that rules the ingestion of food and using average temperature conditions experienced by wild seabass (obtained from tagged individuals), the model was able to reproduce the duration of the different stages, the growth of the individuals, the number of batches and their survival to starvation. We also captured one of the major differences encountered in the life traits of the species: farmed fish mature earlier than wild fish (3 to 4 years old vs. 6 years old on average for females, respectively) probably due to better feeding conditions and higher temperature. We explored the growth and survival of larvae and juveniles by exposing the individuals to varying temperatures and food levels (including total starvation). We show that early life stages of seabass have a strong capacity to deal with food deprivation: the model estimated that first feeding larvae could survive 17 days at 15°C. We also tested individual variability by adjusting the specific maximum assimilation rate and found that larvae and juveniles with higher assimilation capacity better survived low food levels at a higher temperature. We discuss our results in the context of the recent years of poor recruitment faced by European seabass.

1. Introduction

European seabass (*Dicentrarchus labrax*) is a species of high economic value in Europe which production relies primarily on aquaculture (81,852 t in 2016; EUMOFA, 2018) and fishing. Both commercial and recreational anglers target seabass, and fishing pressure has rapidly increased from 2,000 t in the late 1970s to more than 9,000 t in 2006, before becoming stable around 6,000 t in 2013 (ICES, 2012). Since then, the state of the "Northern stock" (one of the four stocks defined by ICES, i.e. Irish Sea, Celtic Sea, English Channel and southern

North Sea) has been worrying, as highlighted by the rapid decline in spawning stock biomass and a series of poor recruitments probably due to continued excessive fishing pressure.

The resilience of fish populations is based on their ability to complete their life cycle and maintain abundance through recruitment (Peck et al., 2014). The recruitment success is partly determined by the reproductive potential of the adults and by the survival rate of early life stages (Chambers & Trippel, 2012), which strongly relies on environmental conditions. According to Houde & Hoyt (1987), eggs, yolk-sac larvae, larvae and juveniles are the most vulnerable stages due to high
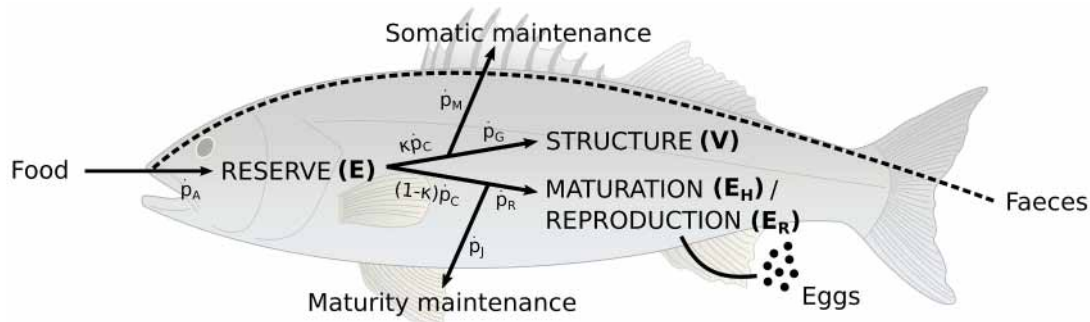
Fig. 1. Schematic representation of the standard DEB model applied to European seabass. Arrows represent energy fluxes (J/d, Table 1). Table 1 records the dynamics of the state variables E, V, E_H and E_R.

rates of predation, starvation and other dietary deficiencies, or to deleterious oceanographic conditions that transport them to unsuitable environments. However, despite their ecological and economical importance, the recruitment dynamics of the European seabass early life stages is still poorly known. Besides, this species is reported to spawn in winter (Fritsch et al., 2007; Pawson et al., 2007), when environmental conditions can be considered as suboptimal in terms of temperature and food availability, which raises questions about eggs and larvae survival during the planktonic phase.

Bioenergetics models are suitable tools to study the impact of environmental variability on the recruitment success of seabass early life stages. They make it possible to study biological and physiological processes on an individual scale in relation to the environment by translating the specific environmental conditions experienced by the fish into individual performance (growth, survival and investment in reproduction). To achieve this, bioenergetics models quantify the energy fluxes between an organism and its environment. In particular, models using the Dynamic Energetic Budget (DEB) theory (Kooijman, 2010) translate an individual's physiological functions into a reduced number of differential equations. It allows the construction of a dynamic model related to the environment without having to conduct laboratory experiments to quantify input (i.e. ingestion and assimilation) and output (i.e. excretion, respiration and locomotion) fluxes as in the Scope For Growth (SFG) models (Winberg, 1956), and it relies only on existing length and weight-at-age data. Besides, in this theory, the rules of energy conservation are followed and the flux of energy to reproduction is explicitly described.

DEB models are commonly used to study some of the fish physiological characteristics (e.g. Jusup et al., 2011), and they are useful to investigate the impacts of environmental changes (i.e. temperature and food availability) on fish growth and reproduction (e.g. Pecquerie et al., 2009 and Pethybridge et al., 2013). Lika et al. (2014) and Stavrakidis-Zachou et al. (2018) successfully parametrized DEB models for seabass. They used data from Mediterranean farmed seabass and focussed on early life stages (i.e. larvae and juveniles). Our primary aim in the present study was, therefore, to develop a DEB model for wild European seabass using full life cycle data. Besides, given the worrying state of the northern stock revealed by ICES, we chose to apply the model to the Northeast Atlantic and to focus on a region stretching from the Bay of Biscay to the English Channel. Preliminary analyses revealed that fitting the model of Stavrakidis-Zachou et al. (2018) to our Northeast Atlantic dataset resulted in an overestimation of seabass growth, particularly for the juveniles (see Supplementary Material). This, along with the recognized genetic differences between Mediterranean and Atlantic populations (Tine et al., 2014) argued for compiling new data and estimating new DEB parameters for wild European seabass.

To reach our aim, we calibrated an 'abj' DEB model using length and weight data, from both farmed (larvae and juveniles) and wild (juveniles and adults) Atlantic specimens. We then evaluated the model's ability to reproduce very distinct life-history traits displayed by farmed

and wild individuals. We applied the model to study two key processes: the growth and survival of early life stages. We evaluated the survival capacity of seabass larvae and juveniles to a range of temperatures and food levels. We also introduced individual variability to study its impact on larval survival in limited food conditions.

2. Material and methods

2.1. The 'abj' DEB model applied to seabass

The standard DEB model (Kooijman, 2010, chapter 2) quantifies the metabolic dynamics of an individual organism during its entire life cycle and describes the processes of growth, maintenance and reproduction. Here, we used an 'abj' model (Marques et al., 2018), which is a standard DEB model with a metabolic acceleration between birth and metamorphosis. Two forcing variables drive the 'abj' model: temperature and food availability. The conversion between food availability and ingestion is obtained using the Holling type II functional response:

$$f = \frac{X}{X_K + X} \tag{1}$$

where X is the food density and X_K the half-saturation constant. f can take values between 0 (food deprivation) and 1 (feeding *ad libitum*).

An individual is described by four state variables: the reserve energy (E, J), the structural volume (V, J), the maturity (E_H, J) - which is the cumulative energy invested to become more complex (i.e. development of new organs, installation of regulation systems; Kooijman, 2010, chapter 2) - and the reproduction buffer (E_R, J). Links between these variables are summarised in Fig. 1. The dynamics of the state variables are described by differential equations (Table 1), which were solved using the finite-difference method with the Euler numerical scheme.

An organism assimilates the food energy following the flux $\dot{p}_A$ (J/d) and added to the energy reserve (molecules waiting to be used to fuel metabolic processes). The stored energy is then mobilised (flux $\dot{p}_C$, J/d) for somatic maintenance and growth with the fraction κ, while the rest (1-κ) is used for maturity maintenance and maturation (juveniles) or reproduction (adults). Maintenance always has priority over the other processes. In other words, if the costs of somatic and/or maturity maintenance cannot be paid from reserve, the individual dies of starvation. Table 1 summarises the equations of the standard DEB model fluxes.

The standard DEB model works for isomorphs, i.e. organisms that do not change in shape. We assume that this is the case during the period from egg to non-feeding larval stages, as well as from juvenile to adult stages. This means that the shape coefficient (δ_M that links the volumetric length (L, cm) and the physical length (L_w, cm) by $L = \delta_M L_w$ (Kooijman, 2010) is constant. For feeding-larvae, the change in shape is given by the shape correction function (Table 1, Augustine et al., 2011) with δ_{Mb} and δ_{Mj} corresponding to the shape coefficients for eggs/non-

Table 1

Equations of the 'abj' model including the dynamics of the four state variables, the metabolic acceleration, the six energy fluxes (J/d) and the shape correction function. Brackets [] represent quantities per unit of structural volume and braces {} represent quantities per unit of structural surface area.

Reserve dynamics	$\frac{dE}{dt} = \dot{p}_A - \dot{p}_C$
Structural length dynamics	$\frac{dL}{dt} = \frac{\dot{p}_G}{3L^2[E_G]}$
Maturity level dynamics	$\frac{dE_H}{dt} = \dot{p}_R$ if $E_H < E_H^p$
	else $\frac{dE_H}{dt} = 0$
Reproductive buffer dynamics	$\frac{dE_R}{dt} = \dot{p}_R$ if $E_H \geq E_H^p$
	else $\frac{dE_H}{dt} = 0$
Metabolic acceleration	if $E_H < E_H^h$ $s_M = 1$
	if $E_H^h \leq E_H < E_H^j$ $s_M = L/L_b$
	if $E_H \geq E_H^j$ $s_M = L_j/L_b$
Assimilation flux	$\dot{p}_A = s_M\{\dot{p}_{Am}\}fL^2$ if $E_H \geq E_H^b$
	else $\dot{p}_A = 0$
Mobilisation flux	$\dot{p}_C = \frac{E}{L^3}\left(\frac{s_M\dot{v}[E_G]L^2 + [\dot{p}_M]L^3}{[E_G] + \frac{\kappa E}{L^3}}\right)$
Somatic maintenance flux	$\dot{p}_M = [\dot{p}_M]L^3$
Growth flux	$\dot{p}_G = \kappa\dot{p}_C - \dot{p}_M$
Maturity maintenance flux	$\dot{p}_J = \dot{k}_J E_H$
Maturation or reproduction flux	$\dot{p}_R = (1-\kappa)\dot{p}_C - \dot{p}_J$
Shape correction function	$\delta_M(L) = \delta_{Mj} + (\delta_{Mb} - \delta_{Mj})\frac{L_j - L}{L_j - L_b}$

feeding larvae and juveniles/adults, respectively, and L_b and L_j corresponding to the volumetric lengths at birth (*sensu* DEB, i.e. mouth opening) and metamorphosis, respectively. L_b and L_j are saved during the simulation and used in post-treatment to calculate the shape correction function (Table 1).

The metabolic acceleration (Table 1) accounts for the exponential growth increase of the larvae until metamorphosis. It affects the maximum surface-area-specific assimilation rate $\{\dot{p}_{Am}\}$ (J.cm^{-2}.d^{-1}) and the energy conductance $\dot{v}$ (cm.d^{-1}), thereby, the acceleration of growth relies on an increasing amount of intake and reserve mobilization during the larval stage.

The temperature affects all the fluxes as enzymatic processes are accelerated within a given temperature range. According to Kooijman (2010), we used the extended Arrhenius relationship to quantify the temperature effect on all fluxes:

$$\dot{k}(T) = \dot{k}(T_1)\exp\left(\frac{T_A}{T_1} - \frac{T_A}{T}\right)\left(\frac{1 + \exp\left(\frac{T_{AL}}{T_1} - \frac{T_{AL}}{T_L}\right) + \exp\left(\frac{T_{AH}}{T_H} - \frac{T_{AH}}{T_1}\right)}{1 + \exp\left(\frac{T_{AL}}{T} - \frac{T_{AL}}{T_L}\right) + \exp\left(\frac{T_{AH}}{T_H} - \frac{T_{AH}}{T}\right)}\right)$$

(2)

with $\dot{k}$ a physiological rate, T the absolute temperature in Kelvin, T_1 a reference temperature of 293.15 K, T_A the Arrhenius temperature, T_L

and T_H the critical lower and upper boundaries of the thermal tolerance range (respectively 10°C and 28°C, in Kelvin in the model), and T_{AL} and T_{AH} the Arrhenius temperatures for these boundaries.

The standard DEB model operates over the entire life cycle and differentiates three life stages: embryo, juvenile and adult. As each one of these DEB stages may include different biological stages, and because we aim to study the early life stages, we considered five life stages: the egg and non-feeding larval stage (does not feed or reproduce, i.e. the embryo *sensu* DEB), feeding larva and juvenile stage (feeds but does not reproduce, i.e. juvenile *sensu* DEB) and the adult stage (feeds and reproduces). Transitions between stages occur at specific thresholds of maturity E_H. An egg hatches at $E_H = E_H^h$, a non-feeding larva starts feeding at $E_H = E_H^b$, the metamorphosis occurs at $E_H = E_H^j$ and a juvenile becomes mature at $E_H = E_H^p$.

During the two first life stages, an individual lives on its reserves ($\dot{p}_A = 0$). After the mouth opening, the flux $\dot{p}_A$ depends on food availability. The energy in reserve (E_0, J) for an egg was estimated at 2.8 J using the biochemical composition of seabass eggs from wild genitors acclimatized to captivity for 4 to 6 years (Devauchelle & Coves, 1988). We acknowledge that genetic selection, as well as experimental conditions, may have modified the energy content of the eggs used in our experiments as compared to the value of Devauchelle & Coves (1988), and that wild eggs may also have different energy content, but with no means of estimating these differences, we used the best available information. Moreover, this value was included in the range proposed by Riis-Vestergaard (2002), who developed a generalization to calculate the energy density of marine pelagic fish eggs by averaging the energy density as a function of the percentage of the oil globule compared to the total egg volume.

As specified in Kooijman (2010, chapter 2), strategies to handle E_R are species-specific and the management of this buffer can be adapted in each DEB model. Hereafter, we summarised the rules used in this model. For adults, the spawning season was set between January and May to cover all potential spawning over the entire study area (from the Bay of Biscay to the English Channel). The energy of one batch is defined as:

$$E_B = N_B E_0 Ww$$

(3)

with N_B the relative batch fecundity ($N_B = 104$ eggs/g of female; Stéphane Lallement, 2018 pers. comm.), E_0 the energy of an egg and W_w the wet weight of the individual:

$$W_w = d_v L^3 + \frac{E}{\rho_E \frac{d_v}{d_{vd}}} + \frac{R}{\rho_R \frac{d_v}{d_{vd}}}$$

(4)

with d_v, d_{vd}, ρ_E and ρ_R as defined in Table 3.

According to (Mayer et al., 1990), seabass can produce between two and four batches per year. For simplicity and because it does not change the seasonal bioenergetic the reproduction buffer was emptied once a year, as soon as it contained enough energy, during the spawning season. Then, this energy was converted into a number of batches following the equation:

$$n = \frac{E_R \kappa_R}{N_B E_0 Ww}$$

(5)

with n the number of batches, κ_R the fraction of reproduction energy fixed in eggs (Table 2) and E_R, N_B, E_0, W_w as defined previously.

In the case of prolonged starvation, various levels of response can be considered (Kooijman, 2010; chapter 4). Here, we chose to continue the standard reserve dynamics until death occurred. The κ-rule for allocation was kept unchanged. No shrinkage occurred.

2.2. Calibration of a model adapted to the Atlantic wild seabass population

2.2.1. Data description

Length-at-age and weight-at-age datasets were used to calibrate the DEB model. Data for wild seabass were available in the Ifremer

Table 2

Comparison of the 15 optimized and 8 fixed DEB parameters used in this study of European seabass with the values published by Stavrakidis-Zachou, et al (2018). All rates are expressed at $T_1 = 293.15$ K ($=20°C$). Brackets [] indicate quantities per unit of structural volume and braces {} indicate quantities per unit of structural surface area.

Symbol	This study (1)	Stavrakidis-Zachou et al.'s model (2)	$\frac{(1)-(2)}{(2)}$	Unit	Definition
κ	0.478	0.56	-0.15	–	Allocation fraction to soma
$\{\dot{p}_{Am}\}$	109.7 / 581.4*	85.44 / 585.85*	0.28 / -0.008*	J.cm^{-2}.d^{-1}	Specific maximum assimilation rate
v'	0.023 / 0.122*	0.041 / 0.282*	-0.44 / -0.57*	cm.d^{-1}	Energy conductance
$[E_G]$	6678	5230	0.28	J.cm^{-3}	Specific costs for structure
$[\dot{p}_M]$	18	19.6	-0.08	J.cm^{-3}.d^{-1}	Volume-specific somatic maintenance rate
T_A	7002	7998	-0.12	K	Arrhenius temperature
E_H^h	0.047	0.14	-0.66	J	Maturity threshold at hatching
E_H^b	0.306	1.61	-0.81	J	Maturity threshold at birth
E_H^j	45.7	526.16	-0.91	J	Maturity threshold at metamorphosis
E_H^p	2507273	2510000	0	J	Maturity threshold at puberty
δ_{Mb}	0.058	/	/	–	Shape coefficient for eggs and non-feeding larvae
δ_{Mj}	0.16	0.148	0.08	–	Shape coefficient for juveniles and adults
T_{AL}	38563	22974	0.68	K	Arrhenius temperature at low boundary
T_{AH}	89833	87590	0.03	K	Arrhenius temperature at high boundary
f	0.833	/	/	–	Scaled functional response for wild data
T_L	283.15 (Claireaux & Lagardère, 1999)	274	0.03	K	Critical lower boundary of thermal tolerance range
T_H	301.15 (Claireaux & Lagardère, 1999)	303	-0.01	K	Critical upper boundary of thermal tolerance range
κ_R	0.95 (Kooijman, 2010)	0.95	0	–	Fraction of reproduction energy fixed in eggs
$\dot{k}_J$	0.002 (Marques et al., 2018)	0.002	0	d^{-1}	Maturity maintenance rate coefficient
ρ_V	23431 (Lika et al., 2011)	23431	0	J.g^{-1}	Energy density for structure
ρ_E	23431 (Lika et al., 2011)	23431	0	J.g^{-1}	Energy density for reserve
d_v	1 (Kooijman, 2010)	1	0	g.cm^{-3}	Specific density of wet structure
d_{vd}	0.2 (Kooijman, 2010)	0.2	0	g.cm^{-3}	Specific density of dry structure

* Values before/after acceleration.

database 'Bargeo'. This database contains all biological measurements and estimated biological parameters (length, weight, age, puberty, sex, etc.) of wild individuals collected for Ifremer at fish markets, by observers at sea, or during scientific cruises catching adult (CGFS and EVHOE) or juvenile (NOURDEM) seabass. Over the period 2000–2016, a total of more than 8,000 individuals (3,402 from the English Channel and 4,948 from the Bay of Biscay) aged between 6 months and 22 years were sampled and considered for this analysis. In the database, the age is provided in years. For the model, age was converted to a value corresponding to the number of days between the day of capture and the hypothesis that the individuals were born on February the 2nd.

Length-at-age and weight-at-age data collected during aquaculture experiments carried out by Ifremer (PFOM/ARN lab) were added to the dataset. Two experiments on larvae and juveniles were considered (Howald et al., 2019); the first with individuals between one week and four years old, fed *ad libitum* at a temperature of 15°C (then varying for juveniles but for sake of simplicity, considered as constant around 15°C for the whole experiment), and the second with individuals between 1 week and 8 months old raised at 20°C and fed *ad libitum*.

2.2.2. Parameters estimation

A fundamental assumption when calibrating the 'abj' DEB model for wild seabass was that the model structure and parameters would be similar between wild and domestic strains. Although genetic selection in aquaculture may have changed the growth pattern of domestic strains, our datasets could not account for such differences between strains. Differences can, therefore, only be explained by variations in the forcing variables (temperature and food availability) that are driving the model.

The calibration process was performed by fitting the growth patterns of three average individuals to two experimental (Howald et al., 2019) and one wild datasets. For the experimental datasets, temperature and food availability were kept constant with the scaled functional response (*f*) equal to 1 (i.e. larvae and juveniles fed *ad libitum*), and a temperature of either 15°C or 20°C, depending on the experiment. For the wild dataset, *f* was unknown and considered as a parameter to

estimate. At this stage, we assumed that *f* does not evolve seasonally for seabass, based on the observation that there was no significant weight evolution over the year in our dataset. For the temperature, we used data collected by wild tagged seabass and published by Heerah et al. (2017) and de Pontual et al. (2018). In these studies, electronic tags recorded, at high frequency (approx. every 90 s), the temperature and depth experienced by 1220 European seabass along the Atlantic French coast between 2010 and 2012, and 2014 and 2016. A maximum of two years of data were recorded due to battery capacity. Our aim with this data was to reconstruct a climatology, as accurate as possible, of the temperatures experienced by adult seabass in the wild. For each day of the year, we averaged the temperature experienced by all individuals with a temperature record (Fig. 2). Annual variations were not taken in consideration because the temperature data did not cover the temporal range of the length and weight-at-age data extracted from the Ifremer database.

For parameter estimation, we used the global estimation method CMAES (Covariance Matrix Adaptation Evolution Strategies) (Bäck & Schwefel, 1993) with the Fortran library pCMALib (Müller et al., 2009). As detailed in Gatti et al. (2017), this method estimates the best set of parameters across the entire parameter space, even in the case of a large number of parameters (15 in this study). The cost function to minimize is the sum of two terms:
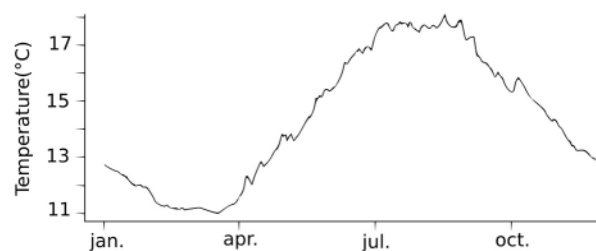

Fig. 2. Temperature climatology reconstructed from tagged seabass, and used for the "wild" dataset during calibration (see Methods).

$$Fcost = \sum_{i}^{datasets} \sum_{j}^{stages} \sum_{k}^{variables} \frac{1}{n_{obs\ i,j,k}} \sum_{l}^{n_{obs\ i,j,k}} \left(\frac{x_{i,j,k,l} - y_{i,j,k,l}}{\sigma_{obs\ i,j,k}} \right)^2$$
$$+ \sum_{m}^{thresholds} \left(\frac{x_m - z_m}{\sigma} \right)^2 \tag{6}$$

The first term represents the fitting of the length- and weight-at-age data for our three datasets, whereas the second term represents the fitting of literature data for length at hatching, mouth opening, metamorphosis and puberty. In the first term, x is the model predictions, y the observations, and $\sigma_{obsi,\ j,\ k}$ and $n_{obsi,\ j,\ k}$, the standard deviations and the number of observations of variable k for stage j and dataset i, respectively. The standard deviations were calculated for each dataset and stage, as it depends on the environmental conditions experienced by the individuals and on their age/length (i.e. the value is linked to the mean). The variables are length and weight, whereas the stages are larvae (both non-feeding larvae and feeding larvae), juveniles and adults. The adult stage lasts much longer than the other stages (fifteen years vs. three months for larvae and six years for juveniles in our calibration) with sizes and weights covering a broad range of values. To better balance the fit with the duration of each stage, we have divided this stage into three equal periods of five to six years (i.e. the duration of the juvenile stage), which has the effect of increasing the weight of the oldest individuals, who are the rarest (i.e. only 46 individuals over 16 years old vs. 1,470 between 11 and 16 years old and 4,800 between 6 and 11 years old). In the second term, x is the length prediction for the different thresholds of E_H, z is the corresponding length at hatching at 15°C (Regner & Dulcic, 1994), mouth opening at 15°C (Kennedy & Fitzmaurice, 1972), metamorphosis in the wild (Barnabé, 1990) and puberty in the wild (Drogou, 2018 pers. comm.), while σ is a standard deviation calculated for length at puberty and set arbitrarily for the others lengths.

As we had no information on reproduction at different food levels, we chose to use the general value for animals following Marques et al. (2018), and set the maturity maintenance rate coefficient, that control the sink of reserve linked to maturity ($\dot{k}_J$, equal to 0.002 d^{-1}). We were also missing information to calibrate the energy density for structure (ρ_V) and reserve (ρ_E). We calculated those parameters by following Lika et al. (2011) and set $\rho_V = \rho_E = 23431$ J.g^{-1}. We also set the specific density of the wet mass (d_v) and dry mass (d_{vd}) at 1 g.cm^{-3} and 0.2 g.cm^{-3}, respectively.

We then optimized 15 parameters: κ, $\{\dot{p}_{Am}\}$, $\dot{v}$, $[E_G]$, $[\dot{p}_M]$, T_A, E_H^h, E_H^b, E_H^j, E_H^p, δ_{Mb}, δ_{Mj}, T_{AL}, T_{AH} and f for the wild dataset. The description of these parameters and their values after optimization are summarised in Table 2 as well as the parameters we set in our model, based on data from the literature. For initializing the model, we used the parameters from Lika et al. (2014). As the parameter T_{AH} modifies the correction factor even before reaching the upper critical temperature T_H, we kept T_{AH} in the list of parameters to be estimated. Claireaux & Lagardère (1999) showed that above 20°C, metabolic fluxes start to decrease; we, therefore, considered that the dataset of larvae raised at 20°C contained information for estimating T_{AH}. Our estimated value appeared very similar to the value of Stavrakidis-Zachou et al. (2018).

2.2.3. Model validation

Seven checks were performed to validate our optimized parameter set in comparison to the literature. First, we checked whether the duration of the egg stage agreed with the literature (Devauchelle & Coves, 1988):

$$D = 414.455 - 119.728lnT \tag{7}$$

with D the incubation duration in hours and T the temperature in degree Celsius. We then checked if birth (*sensu* DEB, i.e. mouth opening) at 19°C and 9°C occurred around 4 and 14 days post-hatching, respectively (Barnabé et al., 1976). We also looked at the survival of larvae without food at 19°C and controlled that the number of batches
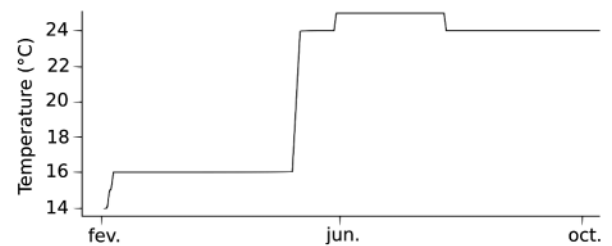

Fig. 3. Temperatures experienced by young seabass in the experiment of Allal et al. (unpublished) and used to validate our DEB model with an independent dataset.

was within the range of two to four batches per year, as shown by in Mayer et al. (1990). Finally, we checked the age at first maturity in aquaculture at 15°C and in the wild, and verified that the growth efficiency

$$\kappa_G = \frac{d_{vd}\rho_v}{[E_G]} \tag{8}$$

was close to 0.8 (Marques et al., 2018) and below 1 (to ensure mass conservation).

For model validation, we used an independent length-at-age and weight-at-age dataset for Atlantic seabass larvae raised in aquaculture since egg fertilization with temperatures varying during the whole experiment (Fig. 3) and individuals fed *ad libitum* ($f = 1$) (Allal et al., unpublished, Ifremer - MARBEC lab). To validate the model, hypothesis tests were made on the parameters of the regression between observed and predicted values for both length and weight.

2.3. Using the model to investigate the effects of varying temperatures and food levels on young seabass

To evaluate the impact of food availability and temperature on the survival of seabass early life stages, we carried out three numerical experiments.

Experiment 1 focused on the ability of young seabass to survive starvation. Here, we numerically analysed the ability to survive starvation as a function of i) the timing of spawning and ii) the state of the individual when food deprivation begins. We considered 12 spawning dates (one for each month of the year) to test the impact of the environment (i.e. mostly temperature) on the survival of young seabass to starvation. We also initiated the food deprivation at four different states (mouth opening and 1, 2 and 3 months after mouth opening) to assess how this affects survival to food deprivation. The temperature was similar to that used for the wild dataset calibration (Fig. 2) and food was set similar to the f calibrated for the wild dataset (Table 2) until starvation begins ($f = 0$).

Experiment 2 numerically investigated whether the life history of larvae during their drift (i.e. the planktonic phase) would have an impact on their survival capacity to starvation once they have reached the nursery. To this end, we tested different scenarios of temperature (10, 15, 20 and 25°C) and food level ($f = 1$ or $f = 0.2$) before starting food deprivation (at 1.2 cm, i.e. the minimal size of larvae observed in English Channel nurseries, Jennings & Pawson, 1992).

Experiment 3 numerically investigated how the environmental conditions affect the growth of seabass larvae and their potential to reach a nursery. Larvae are considered to survive and recruit if, after three to four months (the average drift time according to, Reynolds et al., 2003), they reach a minimum size of 1.2 cm (Jennings & Pawson, 1992). We used the scenario of experiment 2 and the environmental conditions of our "wild" dataset (i.e. the calibrated f and T of Fig. 2) and checked the size of the larvae after 110 days. Some level of individual variability was also introduced in this experiment to assess the properties of our model at an individual scale and evaluate the

sensitivity of the model to variations of one DEB parameter only. Technically, we studied the impact of changing the specific maximum assimilation rate $\{\dot{p}_{Am}\}$ on the growth of larvae. We choose this parameter as the main source of individual variability following the body size scaling relationships defined by the DEB theory (Kooijman, 2010, chap. 8). These body size scaling relationships stipulate that among species, only the specific maximum assimilation rate and the different maturity levels covary with maximum length, the other primary parameters being constant (Kooijman, 2010, chap. 8, Pecquerie et al., 2011). Here, we applied this reasoning to individuals of the same population based on the observed variability of maximum sizes within the population. For each scenario, we simulated 30 individuals with different values of $\{\dot{p}_{Am}\}$. The 30 values were determined to obtain individuals with an asymptotic length ($L_{w\infty}$, Eq. 9) between 58 and 94 cm. The target was a normal distribution centred around 80 cm (the asymptotic length for our study area (Bertignac, 1987).

$$L_{w\infty} = f \frac{L_m}{\delta_{Mj}} = f \frac{\kappa \{\dot{p}_{Am}\} s_M}{[\dot{p}_M]\delta_{Mj}} \tag{9}$$

with f, κ, $\{\dot{p}_{Am}\}$, s_M, $[\dot{p}_M]$ and δ_{Mj} as detailed in Table 2.

3. Results

3.1. Model calibration

The DEB model fitted well our three length-at-age datasets, as illustrated in Fig. 4 for all life stages. For wild larvae, the age in days was not available and our estimation assumed that they were all born in February. This could partly explain why some individuals at the age of about 200 days are longer than others at the age of 500 days (Fig. 4). Another explanation could be inter-annual growth variability.

The model underestimated the weight for all datasets, and Fig. 5 shows that the absolute difference between the model and the data increases with time. The relative difference appeared very variable, with a mean difference of 67% for larvae and 10% for juveniles at 20 °C, and of 13% for larvae and 15% for juveniles at 15 °C. For the wild dataset, the mean difference was 18% for juveniles, 21% for adults 6 to 11 years old, and 6% for the two other groups of adults. We then run a regression between observed and predicted weight values for the first months of life (0–110 days) as we focused on the first life stages. Our results demonstrate that the model reproduces the observations well at 15°C but slightly overestimates the weight at 20°C (Fig. 6). The root-mean-squared errors (RMSE) were 0.007 at 15°C and 0.08 at 20°C. The relative differences for larvae about three to four months old, at 15 and 20°C, were 7% on day 127 and 9% on day 106, respectively. This level of errors was judged acceptable. We thus kept this parameterization for the rest of the study.

Our model was able to produce some interesting results: individuals from aquaculture experiments mature earlier than individuals from the wild (Table 4). This can be seen on the modelled weight curves (Fig. 5) as the curves show sudden stalls when the reproduction occurs (i.e. a batch of eggs is released).

3.2. Model validation

Our model was used to predict a large number of observable properties for which we found corresponding values in the literature. These properties were not used during the calibration procedure and were used as validation data (Table 3). The number of days for the first stages was well reproduced as well as reproduction properties (i.e. number of batches and age at first spawning in different conditions). The survival time was slightly overestimated (i.e. 11 days at 19°C vs. 8 days in experimental conditions).

We also validated our model using an independent dataset of growth data (length and weight) at varying temperatures (Allal et al.,
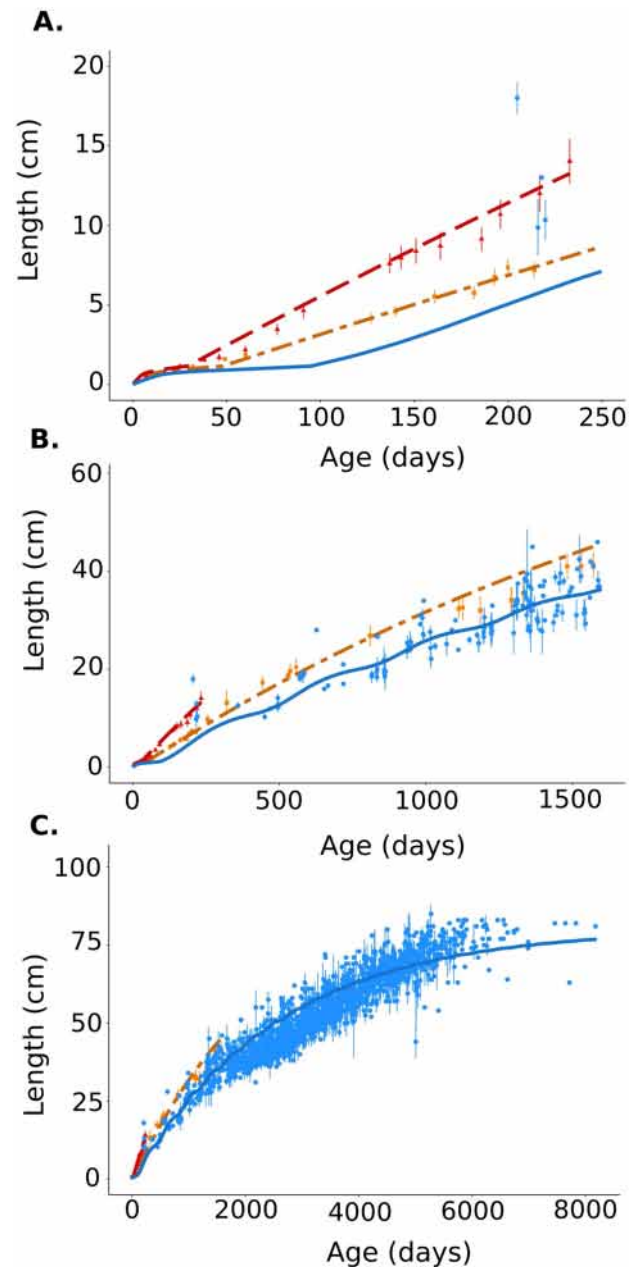

Fig. 4. Model fitted to the three "length-at-age" datasets: A) 0-250 days, B) 0-1,600 days and C) 0-8,200 days. Dots represent mean observations with their standard deviation (not used for calibration). Lines represent model predictions for the aquaculture experiment at 20"C (red), the aquaculture experiment at 15"C (orange), and the "wild" dataset (blue). (For interpretation of the references to colour in this figure legend, the reader is referred to the web version of this article.)

unpublished) (Fig. 7). The model predicted the growth values well with a relative error of 4.4% for length and 7.6% for weight. The regression between observed and predicted values were $y = 0.90x + 0.06$ with $R^2 = 0.99$ for length, and $y = 1.05x + 1.82$ with $R^2 = 0.97$ for weight. The Student's t-test revealed that the intercept was not significantly different from 0. The new equations were $y = 0.90x$ for length and $y = 1.14x$ for weight and the regression validated.

3.3. Survival of larvae and early juveniles to starvation

The ability of larvae and early juveniles to survive starvation was tested at different times of starvation onset (i.e. different spawning
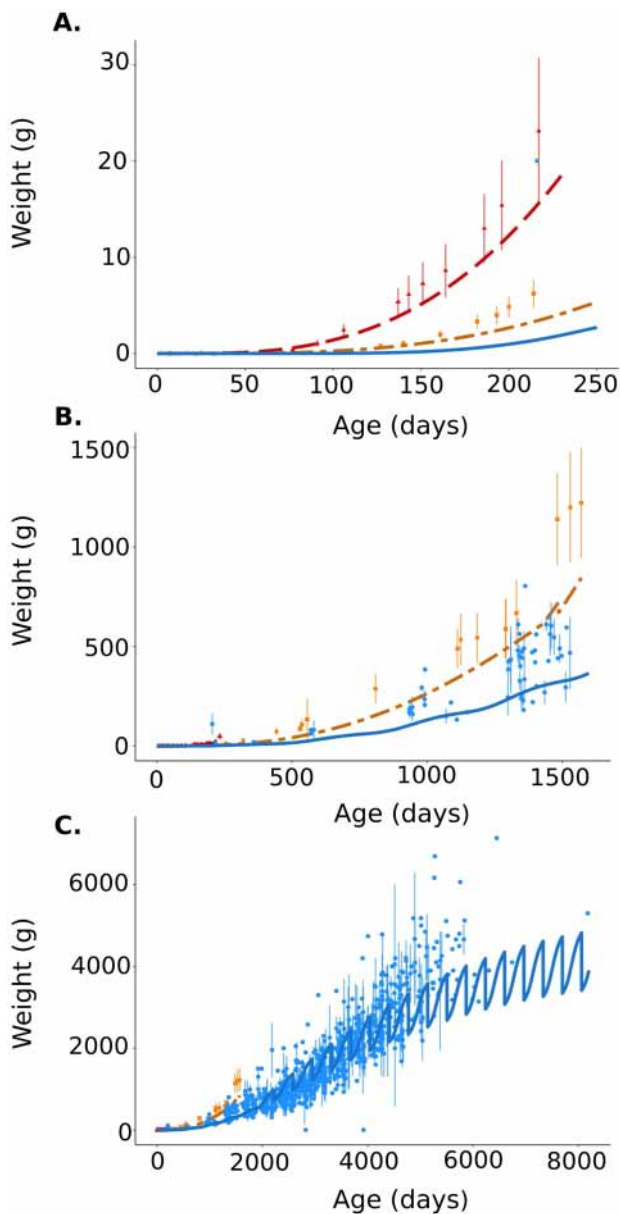
Fig. 5. Model fitted to the three "weight-at-age" datasets: A) 0-250 days, B) 0-1,600 days and C) 0-8,200 days. Dots represent mean observations with their standard deviation (not used for calibration). Lines represent the model predictions for the aquaculture experiment at 20"C (red), the aquaculture experiment at 15"C (orange), and the "wild" dataset (blue). (For interpretation of the references to colour in this figure legend, the reader is referred to the web version of this article.)

months and ages, cf. Experiment 1 and Fig. 8).

Our results demonstrate that the season at which starvation occurs is the main factor explaining the survival of the larvae with the longest survival times occurring when starvation happens in winter (lowest temperatures). Besides, when starvation starts straight at mouth opening, individuals born during the first months of the year appear to survive starvation longer than those born in the middle or at the end of the year (19–34 days vs. 13–22 days). When food deprivation starts at one month old, the same pattern is observed, although slightly shifted towards autumn; larvae appear to endure starvation better between October and April than during the rest of the year (22–33 days vs. around 20 days). On the other hand, if starvation starts at three months old, individuals born during summer and autumn appear more resistant to starvation than the others (16–25 days in July and 22–34 days in

October vs. 12–16 days in April). We also observed that larvae (or juveniles) are more sensitive to starvation when food deprivation starts about two months after birth (blue squares in Fig. 8).

3.4. Effect of temperature and food history on the survival of young seabass

Fig. 9 shows the impact of temperature and food history on the survival of seabass larvae as tested during experiment 2. As implied by the DEB theory, we observed that the survival capacity of larvae decreases with temperature as well as the energy in reserve. At the end of the experiment, larvae fed at $f = 1$ had 46 J on average whereas those fed at $f = 0.2$ had 8 J on average. Our results also indicate that, larvae fed ad libitum ($f = 1$) survive starvation longer than those fed at $f = 0.2$. Finally, the difference in survival time between the two experiments decreased with temperature. The individuals fed *ad libitum* at 10°C surviving 15 days longer than those fed at $f = 0.2$ whereas at 25°C, they survived only 2 more days.

3.5. Effect of temperature, food history and individual variability on the growth of young seabass

Experiment 3 tested the impacts of temperature and food history on the growth of larvae and assessed variability at the individual scale. As explained in the methods, we consider that a larva successfully survived if it reached 1.2 cm in length (the recruitment size) within 110 days. Fig. 10 illustrates the mean sizes reached by the 30 individuals with different $\{\dot{p}_{Am}\}$ in the eight environmental conditions after 110 days. At 10°C, neither the individuals fed *ad libitum*, nor those fed at $f = 0.2$ survived until recruitment. At 15°C, the 30 individuals fed *ad libitum* survived while all the others "died". At 20°C, the 30 individuals fed *ad libitum* all survived, while only seven of those fed at $f = 0.2$ (those with an asymptotic length of more than 84 cm) would have survived the planktonic larval phase (Fig. 11). Finally, at 25°C, all individuals survived in both populations. In the conditions of the "wild" dataset, the seven smaller individuals (i.e. those with an asymptotic length of less than 73 cm) did not survive (Fig. 11).

4. Discussion

The DEB parameters for Atlantic European seabass were estimated with a robust method based on an evolutionary algorithm. The estimation was performed using three Atlantic population datasets: two from aquaculture experiments and one from the wild. Using this approach, we estimated food availability (i.e. the scaled functional response; $f = 0.833$) for the wild individuals of our study area (Bay of Biscay – English Channel). The model predicted a large number of properties, which were in agreement with data from the literature. Notably, farmed individuals appeared to grow faster and reach full maturity earlier than wild individuals, mainly because they are fed *ad libitum* and raised at higher temperatures. The model was then used to carry out three experiments that demonstrated (i) higher starvation survival rates when eggs are hatch in winter, (ii) the importance of food throughout the planktonic phase and (iii) the need of food in spring in nurseries.

For this study, we performed a new parametrization of the European seabass DEB model and compared the parameters to the model of Stavrakidis-Zachou et al. (2018) (Table 2). The two calibrations showed differences in the fish lengths and ages at hatching, birth, metamorphosis and puberty (Table 4). The individuals of the Stavrakidis-Zachou et al. (2018)'s model grow faster: they reach puberty earlier, even if their puberty length is longer (i.e. 53.38 cm against 42 cm). Similarly, we noted differences in lengths at metamorphosis, a stage transition that is complicated to determine and which occurs earlier in individuals with an Atlantic origin. This observation is in agreement with Darias et al. (2008) who highlighted significant changes in the transcriptome of Atlantic seabass larvae at 20°C between days 17 and
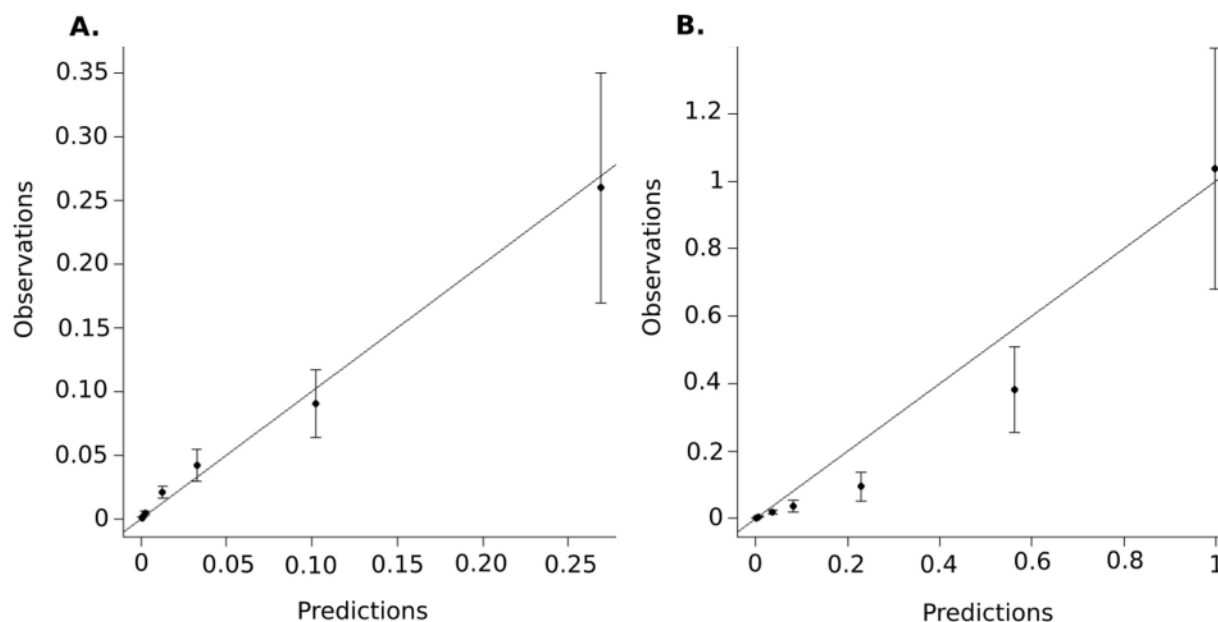
Fig. 6. Plot of observed weight values with their standard deviation error bars (y-axis) vs. predicted weight values (x-axis) compared to the 1:1 line for the 0–110 days time period: A) experiment at 15°C and B) experiment at 20°C.

31 post-hatching, and which could correspond to metamorphosis. Overall, our model improves the predictions of Atlantic seabass growth (in length); however, weight predictions can still be improved.

We used our model to study fish growth in relation to temperature and food availability. Generally, individuals in aquaculture grow faster because they are well fed and raised at higher temperatures (e.g. Person-Le Ruyet et al., 2004), and they reach full puberty earlier (e.g. Pawson, 2000) than wild populations. Our DEB model was able to reproduce these characteristics (Figs. 4 and 5) with an initial spawning at six years old (for females), which is close to previous observations in Atlantic seabass populations (Kennedy & Fitzmaurice, 1972; Pawson & Pickett, 1996), whereas, according to puberty tests, the initial spawning of farmed female seabass is around three to four years old (e.g. Forniés et al., 2001; Servili, 2018 pers. comm.).

We then used the model to explore the effects of selected environmental factors (i.e. food and temperature) on egg and larval biological traits in the wild, including growth and survival. The aim was to provide some understanding of the poor recruitment events experienced by seabass in the Northeast Atlantic since 2010 (ICES, 2018). The spawning season of seabass occurs in winter (Fritsch et al, 2007; Pawson et al, 2007), which was put forward by Warlen & Burke (1990) as an advantage for the migration of the larvae to nurseries. Indeed, drifting larvae encounter fewer predators or competitors for food during winter and when they reach nursery estuaries in spring, temperatures start rising, which allows them to achieve faster growth. However, in winter in our study area, the seawater temperature is colder and phytoplankton and zooplankton are less abundant than

during spring and autumn when planktonic production is the highest (Pingree & Garcia-Soto, 2014). This led us to use our DEB model to assess the effect of temperature and food availability on the growth and survival of early life stages (i.e. planktonic phase) and in the nurseries.

During our first experiment, which tested the ability of seabass larvae to survive food deprivation, we observed that individuals born between January and April-May coped better with total food deprivation than individuals born later (Fig. 8). On the other hand, if starvation starts when larvae reach their nurseries (i.e. at about three to four months old), individuals born at the beginning of the year appear less resistant to starvation (Fig. 8). This means that if spawning takes place in winter, the seabass larvae or young juveniles that reach nurseries in summer need food to survive. With experiment 2, we investigated the impact of temperature and food history during the planktonic phase on starvation survival in the nurseries. Our results indicate that at low temperatures, the food history of the larvae affects their capacity to survive starvation in nurseries (Fig. 9). In the wild, since the drift occurs in winter when food is scarce, the availability of food at nurseries seems to be essential for the survival of the recruits according to our results. These findings indicate that low food levels at nurseries could be one of the factors explaining the poor recruitments observed over the past few years. Besides, according to Martinho et al. (2009) and Vinagre et al. (2009), factors that most influence the good recruitment of seabass in nurseries are high river runoff and heavy rainfall, which probably support planktonic production through nutrients inputs.

With experiment 3, we investigated the impact of temperature and food history during the drift on the growth of seabass larvae. Again, we

Table 3

Quantities derived from the calibrated 'abj' DEB model (f = 0.833) and values from the literature used for comparison and validation.

| Quantities derived from the calibrated model	Value	Literature
Duration of the egg stage (days)	4/3*	3.759/2.324* (Devauchelle & Coves, 1988)
Number of days post-hatching before mouth opening at 15°C	5	7 (Barnabé et al., 1976)
Larval survival at 19°C without food (days)	11	7–8 (Zambonino, 2018 pers. comm.)
Age at first spawning in the wild (years)	6	6 (Kennedy & Fitzmaurice, 1972; Pawson & Pickett, 1996)
Number of batches per year (in the wild)	4	2–4 (Mayer et al., 1990)
Age at first spawning at 15°C (years)	4	4 (Servili, 2018 pers. comm.)
Growth efficiency	0.7	0.8 (Marques et al., 2018)

* Values at 15°C / 20°C.
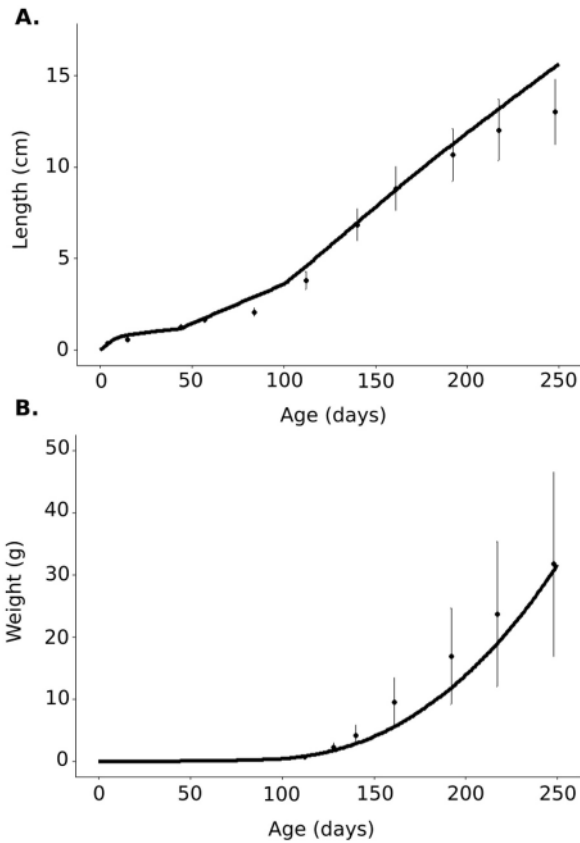
Fig. 7. Validation of our model (line) using an independent dataset (dots with their standard deviation) for A) length and B) weight. Individuals were fed ad libitum and raised at temperatures shown on Fig. 3.
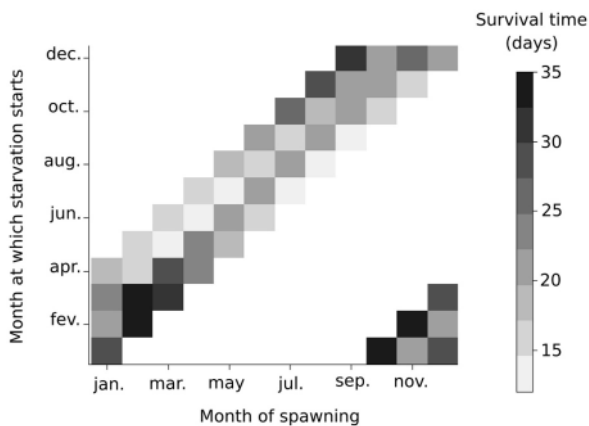

Fig. 8. Experiment 1: Starvation survival time of seabass larvae (in days) relative to the spawning month (x-axis) and the month at which starvation starts (directly at mouth opening, or 1, 2 or 3 months after mouth opening) (y-axis). The feeding level corresponds to f = 0.833 (estimated from the calibration procedure) and the temperature follows Fig. 2.

observed that individuals raised at low temperatures require sufficiently good environmental conditions (i.e. temperature and food) during the first three to four months of their life to grow to size of at least 1.2 cm in length and reach nurseries alive. These results indicate that between 10 and 15°C (i.e. winter temperatures), food availability is a key factor for seabass larvae to grow sufficiently and reach nurseries alive. It is possible that the spawning period of the European seabass may be timed by a trade-off between optimal temperatures and food availability during the drift.
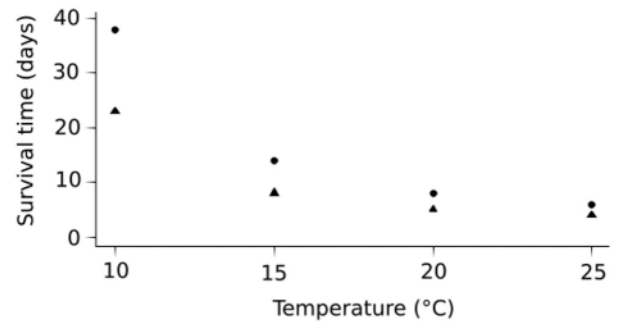

Fig. 9. Experiment 2: Starvation survival time of seabass larvae when food deprivation begins at recruitment size (L = 1.2 cm) according to experimental temperature and feeding history: f = 1 (dots) and f = 0.2 (triangles).
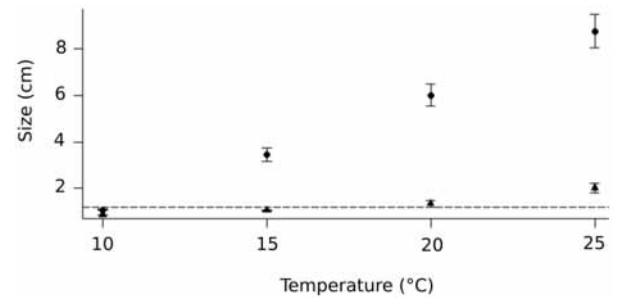

Fig. 10. Experiment 3: Mean sizes and standard deviations for 30 individuals with different $\{\dot{p}_{Am}\}$ according to experimental temperatures and feeding history: f = 1 (dots) and f = 0.2 (triangles). The dotted line represents the target size of 1.2 cm.
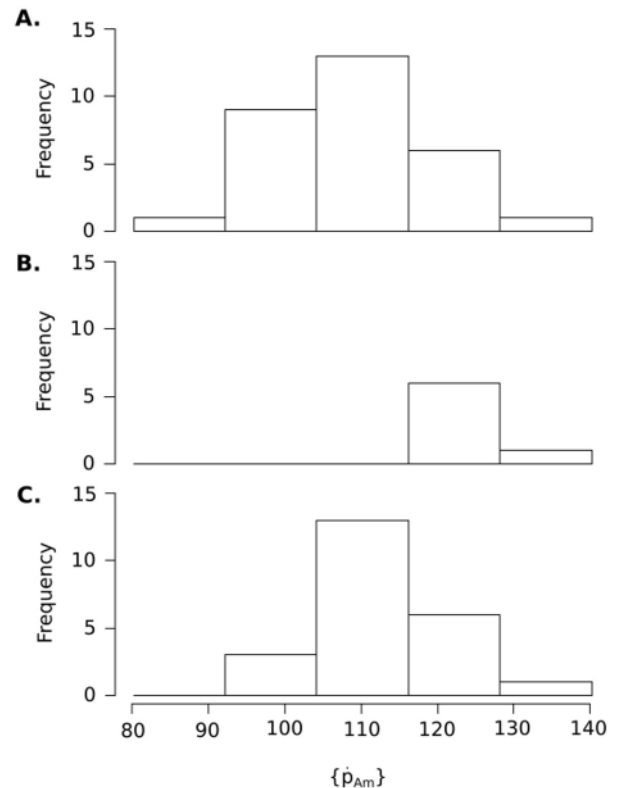

Fig. 11. Experiment 3: Distribution of individuals according to their specific maximum assimilation rate. A) initial population; B) and C) individuals that would have reached at least 1.2 cm-long on day 110 and either fed at f = 0.2 and raised at 20°C (B) or fed and raised using the environmental conditions experienced by the wild dataset (i.e. calibrated f and T as shown in Fig. 2) (C).

Table 4

Comparison of lengths and ages at hatch, birth, metamorphosis and puberty, as predicted using the parameters of this study (wild seabass), with those of farmed seabass (Stavrakidis-Zachou et al., 2018).

	This study	Stavrakidis-Zachou et al., 2018
Length at hatching (cm)	0.32	0.22
Length at birth (cm)	0.58	0.5
Length at metamorphosis (cm)	1.2	3.4
Length at puberty (cm)	42	53.38
Age at hatch at 15 °C (d)	5	3.92
Age at birth at 19 °C (dph)	6	6
Age at metamorphosis at 19 °C (dph)	34	70
Age at puberty at 19 °C (d)	959	723

Introducing individual-scale variability in experiment 3 did not significantly change the effect of environmental conditions. Fig. 10 shows that at 10, 15 and 25°C, the variability inserted in the simulation did not change the model response and all individuals either survived or died. On the other hand, at 20°C, the response varied depending on the individual assimilation rate. Fig. 11 shows that at a very low food level, only individuals with high assimilation capacity (i.e. high $\{\dot{p}_{Am}\}$) can survive a drift at 20°C. In the context of climate change with rising temperatures and lower food level in the North Atlantic (Bopp et al., 2013), our results tend to suggest that individuals with a higher assimilation rate will be better able to recruit than others.

5. Conclusion

For the first time, a DEB model was calibrated for Northeast Atlantic wild European seabass. The use of aquaculture experiments and wild population datasets for calibration provided a robust estimation of the DEB parameters. Our original approach reproduce known traits differences between wild seabass and farmed seabass, with the latter growing faster and reaching full puberty earlier. Food availability is a model input which is difficult to assess in the wild. However, through our calibration procedure, we were able to calculate an estimate showing that wild individuals are not fed *ad libitum*. The model also provided evidence of the seabass' tolerance to temperature and food level variations, confirming the adaptation of this fish to winter spawning in the open ocean. Indeed, in our model, larvae were able to survive long-term food deprivation. We related it to their capacity to survive a drift of about three months with difficult environmental conditions (i.e. low temperature and low food levels). We also stress the need for abundant food in the nurseries for the survival of individuals and suggest that a lack of food could explain the low recruitment of the past years. The future application of this model is to link it to a spatially explicit model at the individual scale to study the connectivity between different seabass functional areas and in particular, between spawning areas and nurseries.

Declaration of Competing Interest

The authors declare that they have no known competing financial interests or personal relationships that could have appeared to influence the work reported in this paper.

Acknowledgments

Supplementary materials

Supplementary material associated with this article can be found, in the online version, at doi:10.1016/j.ecolmodel.2020.109007.

References

Augustine, S., Gagnaire, B., Floriani, M., Adam-Guillermin, C., Kooijman, S.A.L.M., 2011. Developmental energetics of zebrafish, Danio rerio. Comp. Biochem. Physiol. A Mol. Integr. Physiol. 159, 275–283. https://doi.org/10.1016/j.cbpa.2011.03.016.

Bäck, T., Schwefel, H.-P., 1993. An overview of Evolutionary Algorithms for Parameter Optimization. Evol. Comput. 1, 1–23.

Barnabé, G., Boulineau-Coatanea, F., Rene, F., 1976. Chronologie de la morphogenese chez le loup ou bar Dicentrarchus labrax (L.) (Pisces, Serranidae) obtenu par reproduction artificielle. Aquaculture 8, 351–363. https://doi.org/10.1016/0044-8486(76)90117-4.

Barnabé, G., 1990. Rearing bass and gilthead bream. In: Barnabé, G. (Ed.), Aquaculture. Ellis Horwood, New York, pp. 647–686.

Bertignac, M., 1987. L'exploitation Du Bar (Dicentrarchus labrax) Dans Le Morbras (Bretagne Sud). Ecole Nationale Supérieure Agronomique, Laboratoire de biologie halieutique.

Bopp, L., Resplandy, L., Orr, J.C., Doney, S.C., Dunne, J.P., Gehlen, M., ..., Tjiputra, J., 2013. Multiple stressors of ocean ecosystems in the 21st century: projections with CMIP5 models. Biogeosciences 10, 6225–6245.

Chambers, R.C., Trippel, E.A. (Eds.), 2012. Early Life History and Recruitment in Fish Populations 21 Springer Science & Business Media.

Claireaux, G., Lagardère, J.P., 1999. Influence of temperature, oxygen and salinity on the metabolism of the European sea bass. J. Sea Res. 42 (2), 157–168.

Darias, M.J., Zambonino-Infante, J.L., Hugot, K., Cahu, C.L., Mazurais, D., 2008. Gene expression patterns during the larval development of European sea bass (Dicentrarchus labrax) by microarray analysis. Mar. Biotechnol. 10 (4), 416–428.

de Pontual, H., Lalire, M., Fablet, R., Laspougeas, C., Garren, F., Martin, S., ..., Woillez, M., 2018. New insights into behavioural ecology of European seabass off the West Coast of France: implications at local and population scales. ICES J. Mar. Sci. 76 (2), 501–515.

Devauchelle, N., Coves, D., 1988. The characteristics of sea bass (Dicentrarchus labrax) eggs: description, biochemical composition and hatching performances. Aquat. Living Resour. 1, 223–230. https://doi.org/10.1051/alr:1988022.

EUMOFA., 2018. Le marché européen du poisson.

Forniés, M.A., Mañanós, E., Carrillo, M., Rocha, A., Laureau, S., Mylonas, C.C., ..., Zanuy, S., 2001. Spawning induction of individual European sea bass females (Dicentrarchus labrax) using different GnRHa-delivery systems. Aquaculture 202 (3–4), 221–234.

Fritsch, M., Morizur, Y., Lambert, E., Bonhomme, F., Guinand, B., 2007. Assessment of sea bass (Dicentrarchus labrax, L.) stock delimitation in the Bay of Biscay and the English Channel based on mark-recapture and genetic data. Fish. Res. 83, 123–132.

Gatti, P., Petitgas, P., Huret, M., 2017. Comparing biological traits of anchovy and sardine in the Bay of Biscay: A modelling approach with the Dynamic Energy Budget. Ecol. Modell. 348, 93–109. https://doi.org/10.1016/j.ecolmodel.2016.12.018.

Heerah, K., Woillez, M., Fablet, R., Garren, F., Martin, S., De Pontual, H., 2017. Coupling spectral analysis and hidden Markov models for the segmentation of behavioural patterns. Mov. Ecol. 5, 20. https://doi.org/10.1186/s40462-017-0111-3.

Houde, E.D., Hoyt, R., 1987. Fish early life dynamics and recruitment variability. Trans. Am. Fish. Soc.

Howald, S., Cominassi, L., Le Bayon, N., Claireaux, G., Mark, F.C., 2019. Future ocean warming may prove beneficial for the northern population of European seabass, but ocean acidification does not. bioRxiv, 568428.

ICES., 2012. Report of the Working Group for the Celtic Seas Ecoregion (WGCSE), 9– 18 May 2012, Copenhagen, Denmark. ICES CM 2012/ACOM:12. 1715 pp.

ICES., 2018. Report of the Working Group on Celtic Seas Ecoregion (WGCSE), 9–18 May 2018, Copenhagen, Denmark. ICES CM 2018/ACOM:13. 1887 pp.

Jennings, S., Pawson, M.G., 1992. The origin and recruitment of bass, Dicentrarchus labrax, larvae to nursery areas. J. Marine Biol. Assoc. U. K. 72 (1), 199–212.

Jusup, M., Klanjscek, T., Matsuda, H., Kooijman, S., 2011. A full lifecycle bioenergetic model for bluefin tuna. PLoS ONE 6, e21903.

Kennedy, M., Fitzmaurice, P., 1972. The Biology of the Bass, Dicentrarchus Labrax, in Irish Waters. J. Marine Biol. Assoc. U. K. 52, 557–597. https://doi.org/10.1017/S0025315400021597.

Kooijman, B., Kooijman, S.A.L.M., 2010. *Dynamic Energy Budget Theory for Metabolic Organisation.* Cambridge university press.

Lika, K., Kearney, M.R., Freitas, V., van der Veer, H.W., van der Meer, J., Wijsman, J.W.M., Pecquerie, L., Kooijman, S.A.L.M., 2011. The "covariation method" for estimating the parameters of the standard Dynamic Energy Budget model I: Philosophy

and approach. J. Sea Res. 66, 270–277. https://doi.org/10.1016/j.seares.2011.07. 010.

Lika, K., Kooijman, S.A.L.M., Papandroulakis, N., 2014. Metabolic acceleration in Mediterranean Perciformes. J. Sea Res. 94, 37–46. https://doi.org/10.1016/j.seares. 2013.12.012.

Marques, G.M., Augustine, S., Lika, K., Pecquerie, L., Domingos, T., Kooijman, S.A., 2018. The AmP project: comparing species on the basis of dynamic energy budget parameters. PLoS Comput. Biol. 14 (5), e1006100.

Martinho, F., Dolbeth, M., Viegas, I., Teixeira, C.M., Cabral, H.N., Pardal, M.A., 2009. Environmental effects on the recruitment variability of nursery species. Estuar. Coast. Shelf Sci. 83, 460–468. https://doi.org/10.1016/j.ecss.2009.04.024.

Mayer, I., Shackley, S.E., Witthames, P.R., 1990. Aspects of the reproductive biology of the bass, Dicentrarchus labrax L. II. Fecundity and pattern of oocyte development. J. Fish Biol. 141–148.

Müller, C.L., Ofenbeck, G., Baumgartner, B., Schrader, B., Sbalzarini, I.F., 2009. pCMALib: a parallel FORTRAN 90 library for the evolution strategy with covariance matrix adaptation. In: Proc. ACM Genetic and Evolutionary Computation Conference (GECCO'09). Montreal, Canada.

Pawson, M., 2000. The influence of temperature on the onset of first maturity in sea bass. J. Fish Biol. 56, 319–327. https://doi.org/10.1006/jfbi.1999.1157.

Pawson, M.G., Pickett, G.D., 1996. The Annual Pattern of Condition and Maturity in Bass, Dicentrarchus Labrax, in Waters Around England and Wales. J. Marine Biol. Assoc. U. K. 76, 107. https://doi.org/10.1017/S0025315400029040.

Pawson, M.G., Pickett, G.D., Leballeur, J., Brown, M., Fritsch, M., 2007. Migrations, fishery interactions, and management units of sea bass (Dicentrarchus labrax) in Northwest Europe. ICES J. Mar. Sci. 64, 332–345.

Peck, N., Essington, T., Takasuka, G., Dickey-Collas, A., Ravn-Jonsen, V., Kvamsdal, G., Link, R., 2014. Forage Fish Interactions: a symposium on "Creating the tools for ecosystem-based management of marine resources" ICES J. Mar. Sci. 71 (1), 1–4. https://doi.org/10.1093/icesjms/fst174.

Pecquerie, L., Petitgas, P., Kooijman, S.A.L.M., 2009. Modeling fish growth and reproduction in the context of the Dynamic Energy Budget theory to predict environmental impact on anchovy spawning duration. J. Sea Res. 62, 93–105. https://doi. org/10.1016/j.seares.2009.06.002.

Pecquerie, L., Johnson, L.R., Kooijman, S.A.L.M., Nisbet, R.M., 2011. Analyzing variations in life-history traits of Pacific salmon in the context of Dynamic Energy Budget (DEB) theory. J. Sea Res. 66, 424–433.

Person-Le Ruyet, J., Mahé, K., Le Bayon, N., Le Delliou, H., 2004. Effects of temperature on growth and metabolism in a Mediterranean population of European sea bass, Dicentrarchus labrax. Aquaculture 237, 269–280. https://doi.org/10.1016/j. aquaculture.2004.04.021.

Pethybridge, H., Roos, D., Loizeau, V., Pecquerie, L., Bacher, C., 2013. Responses of European anchovy vital rates and population growth to environmental fluctuations: An individual-based modeling approach. Ecol. Modell. 250, 370–383. https://doi. org/10.1016/j.ecolmodel.2012.11.017.

Pingree, R.D., Garcia-Soto, C., 2014. Plankton blooms, ocean circulation and the European slope current: response to weather and climate in the Bay of Biscay and W English Channel (NE Atlantic). Deep Sea Res. Part II 106, 5–22.

Regner, S., Dulčić, J., 1994. Growth of sea bass, Dicentrarchus labrax, larval and juvenile stages and their otoliths under quasi-steady temperature conditions. Mar. Biol. 119 (2), 169–177.

Reynolds, W.J., Lancaster, J.E., Pawson, M.G., 2003. Patterns of spawning and recruitment of sea bass to Bristol Channel nurseries in relation to the 1996 'Sea Empress' oil spill. J. Marine Biol. Assoc. U. K. 83 (5), 1163–1170.

Riis-Vestergaard, J., 2002. Energy density of marine pelagic fish eggs. J. Fish Biol. 60, 1511–1528. https://doi.org/10.1111/j.1095-8649.2002.tb02444.x.

Stavrakidis-Zachou, O., Papandroulakis, N., Lika, K., 2018. A DEB model for European sea bass (Dicentrarchus labrax): Parameterisation and application in aquaculture. J. Sea Res. https://doi.org/10.1016/j.seares.2018.05.008.

Tine, M., Kuhl, H., Gagnaire, P.-A., Louro, B., Desmarais, E., Martins, R.S.T., Hecht, J., Knaust, F., Belkhir, K., Klages, S., Dieterich, R., Stueber, K., Piferrer, F., Guinand, B., Bierne, N., Volckaert, F.A.M., Bargelloni, L., Power, D.M., Bonhomme, F., Canario, A.V.M., Reinhardt, R., 2014. European sea bass genome and its variation provide insights into adaptation to euryhalinity and speciation. Nat. Commun. 5, 5770.

Vinagre, C., Santos, F.D., Cabral, H.N., Costa, M.J., 2009. Impact of climate and hydrology on juvenile fish recruitment towards estuarine nursery grounds in the context of climate change. Estuar. Coast. Shelf Sci. 85, 479–486. https://doi.org/10.1016/j. ecss.2009.09.013.

Warlen, S.M., Burke, J.S., 1990. Immigration of Larvae of Fall/Winter Spawning Marine Fishes into a North Carolina Estuary. Estuaries 13, 453. https://doi.org/10.2307/ 1351789.

Winberg, G.G., 1956. Rate of metabolism and food requirements of fish. Fish. Res. Board Can. Transl. Ser. 194, 1–253.